01 Aug 1977

High Spin-low Spin Crossover and Antiferromagnetic Interactions in Tris(1-pyrrolidinecarbodithioato)iron(III) and the 4-morpholine (FeM) and Dibutyl Analogs, Effect of Recrystallization Solvent, and Crystal Structure of FeM·nitrobenzene

Edward J. Cukauskas

Bascom Sine Deaver

Ekkehard Sinn
Missouri University of Science and Technology

High spin–low spin crossover and antiferromagnetic interactions in tris(1-pyrrolidinecarbodithioato)iron(III) and the 4-morpholine (FeM) and dibutyl analogs, effect of recrystallization solvent, and crystal structure of FeM·nitrobenzene

E. J. Cukauskas, B. S. Deaver, Jr., and E. Sinn

Departments of Physics and Chemistry, University of Virginia, Charlottesville, Virginia 22901
(Received 28 February 1977)

High sensitivity magnetic susceptibility determinations, especially in the range 1.2–4.2 K on pure and dilute tris(pyrrolidinecarbodithioato)iron(III) (FeP) in its high spin form, show that a maximum at about 2 K is caused by antiferromagnetic interactions. The analogous chromium(III) complex does not exhibit significant antiferromagnetism compared to that of the iron complex, and it is likely that the upper e electrons possessed by the iron and not by the chromium are responsible for the bulk of the antiferromagnetism. As the iron atoms are about 9 Å apart in discrete molecules, the antiferromagnetic interactions presumably occur between unpaired spins delocalized on to the ligands of adjacent molecules. This is in keeping with NMR evidence that spin delocalization is greater in the iron(III) than in the chromium(III) complex. When diluted with large amounts of the cobalt(III) analog (CoP), FeP exhibits a spin state equilibrium. Thus, the structure of the FeP molecule is modified slightly (presumably with shortening of the Fe–S bond) to approach that of the CoP host lattice, which has a shorter metal–sulfur bond. The previous history of the samples of ferric dithiocarbamate complexes is shown to be far more important than had previously been suspected: When crystallized from benzene, FeP exhibits a high spin–low spin equilibrium, in constrast with the pure high spin behavior of the complex when not crystallized from benzene. The effect of adding 7% of benzene to the lattice is much greater than that of adding 50% of CoP. The dibutyl analog shows similar effects. The tris(4-morpholinecarbodithioato-S,S')iron(III) complex FeM is shown, by single crystal x-ray data, to contain short Fe–S bond lengths (average 2.353 Å) when recrystallized from nitrobenzene. This indicates that the complex is principally low spin, in keeping with the observed magnetism and with the general strong solvent effect on the spin state. It is now proposed that the difference in Fe–S bond lengths between FeP crystallized from chloroform and FeP from benzene (the reverse of the expected differences) is due to experimental error. Crystal data for FeM·nitrobenzene: space group $P2_1/c$, $Z = 4$, $a = 9.713(3)$ Å, $b = 31.419(8)$ Å, $c = 9.718(2)$ Å, $\beta = 105.04(2)°$, $V = 2864$ Å^3, $R = 3.3\%$, 2712 reflections.

INTRODUCTION

Iron(III) dithiocarbamate complexes derived from secondary amines have a $^2T_2$ (low spin) ground state with a thermally accessible $^6A_1$ state, in all cases studied,[1–12] with the single exception of the pyrrolidyldithiocarbamate [tris(tetramethylenecarbodithioato-S,S')iron(III), FeP, Fig. 1], for which a high spin ($^6A_1$) ground state has been observed.[2,4,13] These data were complicated by the suggestion that when FeP is crystallized from benzene the resulting compound FeP · $(C_6H_6)_{1/2}$, which contains uncoordinated benzene in the lattice,[14] is no longer high spin. Instead a high spin–low spin crossover is observed,[13] as in the other ferric dithiocarbamates.

As a consequence of the high spin–low spin crossover, the dithiocarbamates generally have a magnetic susceptibility maximum near or above liquid nitrogen temperature. Yet the high spin form of FeP itself also has such an anomaly, but at around 2 K.[13] Several mechanisms, or groups of mechanisms, might be responsible for this *a priori*: a high spin–low spin thermal equilibrium, a relatively large positive D term, paramagnetic saturation, and antiferromagnetic interactions. Thus, a full investigation of this complex requires a technique using a negligibly small magnetic field to eliminate saturation effects, yet possessing high sensitivity in order to examine dilute samples in which any antiferromagnetic coupling is minimized. Elimination or evaluation of these mechanisms will permit the other possibilities to be examined. New techniques using superconducting devices satisfy these requirements and a detailed magnetic study of FeP using these techniques is reported here. Further evidence of the effect of benzene or other solvent molecules included in the lattice is provided by the closely related complex tris(4-morpholinecarbodithioato-S,S')iron(III), FeM; the "unsolvated" complex, as well as the chloroform, dichloromethane, and water solvates, are mostly high spin at

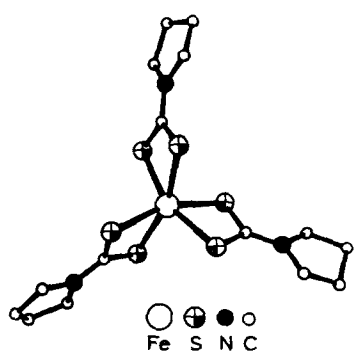

FIG. 1. The FeP molecule. FeM is similar, with the NC_4H_8 ring replaced by a NC_4H_8O ring. $FeBu_2$ has the ring replaced by two n-butyl groups.

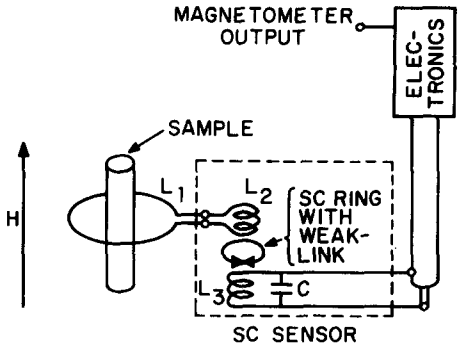

FIG. 2. Schematic diagram of the susceptibility apparatus.

room temperature and have long Fe–S bonds, while the benzene solvate is mostly low spin at room temperature and has short Fe–S bonds. We find that the nitrobenzene solvate FeM · Nbz is also predominantly low spin at room temperature. Thus, a study of the structural and magnetic properties of this complex has been undertaken to help elucidate how such solvent molecules promote low spin states.

EXPERIMENTAL

Susceptibility apparatus

Magnetic susceptibility measurements were made using a superconducting susceptometer incorporating a sensitive Josephson junction magnetometer, superconducting magnets, and shields. The details of the apparatus along with its limitations and potential have recently been discussed.[15]

The scheme used for measuring susceptibility is illustrated by Fig. 2. The magnetometer consists of a superconducting thin film ring interrupted by a single Josephson junction inductively coupled to an rf tank circuit resonant at 30 MHz. This device is often referred to as an rf SQUID and is operated using the original technique developed by Silver and Zimmerman.[16] External flux is coupled to the SQUID by the superconducting flux transformer L_1–L_2. These flux changes are recorded as persistent currents which are coupled to the SQUID and appear as a modulation on the rf drive current with period equal to one flux quantum $\phi_0 = h/2e = 2.07 \times 10^{-7}$ G cm^2. The magnetometer is most often used as a null detector by applying a small audio frequency flux and using phase sensitive techniques.

The static magnetic field was provided by a superconducting solenoid operated in a persistent current mode and stabilized to better than one part in 10^{14}/s by a superconducting shield located just inside and concentric with the magnet. The sample was isolated from the low temperature environment by a silvered quartz Dewar.

The sensitivity of the system has been measured to be better than 10^{-10} cgs with a 1 cm^3 sample. The major source of noise is accounted for by Johnson noise and fluctuations in nuclear paramagnetism of the copper construction material in the 4 K environment. This limitation is eliminated in an improved design which should make possible an increase of sensitivity of several orders of magnitude.

Magnetic measurements

The superconducting susceptometer has the unique feature of an absolute calibration independent of any secondary standards. The system described above was calibrated to an accuracy of 1% by applying a known flux inside the pickup loop L_1 with a carefully characterized long cylindrical coil. Samples were prepared for measurement by packing in long cylindrical quartz tubes with inside diameters ranging from 1–4 mm in order to use the direct calibration. The samples were first purged of all air by replacement with helium before inserting into the liquid helium-filled Dewar. Immediately above the sample and in thermal equilibrium with the sample and liquid helium was mounted a carbon resistance thermometer.

Measurements were made by two methods. The first method involved inserting (or removing) the sample from the pickup loop by means of a motorized rack and pinion connected to the sample positioning rod. The flux change when the sample is inserted is proportional to the susceptibility at the fixed temperature. The second method entails pumping up the liquid helium in the sample Dewar while the sample is coupled to the pickup loop L_1 and plotting the magnetometer output versus the resistance of the carbon thermometer. This method gives a continuous plot of susceptibility versus temperature over the liquid helium range. Both methods have been used and give agreement to within 1%. The magnetic field was determined by measuring the proton NMR of a delrin rod and assuming a resonance frequency of 4.2577 KHz/G. This yielded a field measurement to an accuracy of $\pm\frac{1}{2}$%. Measurements above 4 K were made using an isolating cryostat to separate the sample from the magnetometer. Measurements down to 4 °K were also carried out on a Foner vibrating sample magnetometer.[17] We are grateful to Professor H. B. Gray for access to this instrument. The applied field was varied from 115 Oe to 10 KOe, but most of the measurements were made at 115 Oe.

Preparation of complexes

Iron(III), chromium(III), and cobalt(III) pyrrolidyl dithiocarbamates and iron(III) morpholyl (FeM) and di-*n*-butyl (FeBu) dithiocarbamates were prepared using standard methods[1,2,6,14,18,19] by reacting carbon bisulfide and pyrrolidine or morpholine with freshly prepared ferric hydroxide, chromium(II) chloride, or sodium *tris*[carbonatocobaltate(III)] in air. The benzene solvates FeP · $(C_6H_6)_{1/2}$ and $FeBu_2 \cdot (C_6H_6)$ were prepared as previously described.[12,14] Mass spectral, NMR, x-ray diffraction, and magnetic susceptibility measurements were used to establish the purity of the complexes. The diluted samples of iron(III) in the cobalt(III) complex were prepared by recrystallization from the appropriate mixtures of FeP and CoP dissolved in chloroform solution to which ethanol was added very slowly. The resulting crystals varied from lustrous black to dark green depending on the proportion of cobalt(III).

Analogous dithiocarbamate complexes of trivalent transition metals such as Fe, Co, and Cr have been observed to be isomorphous in the many cases examined so far.[8,9,20,21] as are most of the dtc complexes of these metals, and cocrystallization occurs readily. Like many other dithiocarbamate complexes CrP, FeP, and CoP readily form solids which contain molecules of solvent. From benzene the crystallized solvate contains half a molecule of solvent per complex molecule, and the structures of these crystals are known.[14] From chloroform the complexes crystallize with one molecule of solvent per complex molecule, but the crystal structures are not yet known. Only the ferric complex loses chloroform rapidly, and measurable amounts are lost in a few hours, while heating for several days above 100 °C is required to remove all the solvent from the other complexes.

X-ray crystallography

The crystal for x-ray diffraction was obtained as described previously[9] and sealed in a glass capillary. Crystal data for FeM · Nbz were: $FeS_6O_5N_4C_{21}H_{29}$, $M = 665.7$, space group $P2_1/c$, $Z = 4$, $a = 9.713(3)$ Å, $b = 31.419(8)$ Å, $c = 9.718(2)$ Å, $\beta = 105.04(2)°$, $V = 2864$ Å^3, $\mu(MoK\alpha) = 9.9$ cm^{-1}, $d_{calc.} = 1.53$ g cm^{-3}, $d_{obs.} = 1.54$ g cm^{-3}; crystal dimensions (distances in mm from centroid): (110) 0.05; (1$\bar{1}$0) 0.06; (0.10) 0.10; (0$\bar{1}$0) 0.10; (001) 0.10; (00$\bar{1}$) 0.10.

The Enraf–Nonius program SEARCH was used to obtain 15 accurately centered reflections which were then used in the program INDEX to obtain approximate cell dimensions and an orientation matrix for data collection. Refined cell dimensions and their estimated standard deviations were obtained from least squares refinement of 28 accurately centered reflections. The mosaicity of the crystal was examined by the ω-scan technique and judged to be satisfactory.

Collection and reduction of the data

Diffraction data were collected at 292 K on an Enraf–Nonius four-circle CAD-4 diffractometer controlled by a PDP 8/M computer, using Mo$K\alpha$ radiation from a highly oriented graphite crystal monochromator, as previously described.[9,22] The θ–2θ scan technique was used to record the intensities for all nonequivalent reflections for which $1° < 2\theta < 48°$. Scan widths (SW) were calculated from the formula $SW = A + B\tan\theta$, where A is estimated from the mosaicity of the crystal and B allows for the increase in width of peak due to $K\alpha_1$ and $K\alpha_2$ splitting. The values of A and B were 0.6 and 0.2°, respectively. Reflection data were considered insignificant if intensities registered less than 10 counts above background on a rapid prescan, such reflections being rejected automatically by the computer.

The intensities of four standard reflections, monitored at 100 reflection intervals, showed no greater fluctuations during the data collection than those expected from Poisson statistics. The raw intensity data were corrected for Lorentz-polarization effects (including the polarization effect of the crystal monochromator) and then for absorption. After averaging the intensities of equivalent reflections the data were reduced to 3467 independent intensities of which 2712 had $F_0^2 > 3\sigma(F_0^2)$, where $\sigma(F_0^2)$ was estimated from counting statistics.[23] These data were used in the final refinement of the structural parameters.

Determination and refinement of the structure

The iron and sulfur atoms were located from a three dimensional Patterson synthesis. Full-matrix least-squares refinement was based on F, and the function minimized was $\sum w(|F_0| - |F_c|)^2$. The weights w were then taken as $[2F_0/\sigma(F_0^2)]^2$, where $|F_0|$ and $|F_c|$ are the observed and calculated structure factor amplitudes, respectively. The atomic scattering factors for nonhydrogen atoms were taken from Cromer and Waber,[24] and those for hydrogen from Stewart *et al.*[25] The effects of anomalous dispersion for all nonhydrogen atoms were included in F_c using the values of Cromer and Ibers[26] for $\Delta f'$ and $\Delta f''$. Agreement factors are defined as $R = \sum||F_0| - |F_c||/\sum|F_0|$ and $R_w = (\sum w(|F_0| - |F_c|)^2/\sum w|F_0|^2)^{1/2}$. The intensity data were phased sufficiently well by the metal and sulfur positions to permit location of the remaining nonhydrogen atoms by difference Fourier syntheses. The model converged with $R = 8.9\%$. Further difference Fourier syntheses now revealed the position of all hydrogen atoms which were then included in the calculation. Anisotropic temperature factors were introduced for all nonhydrogen atoms. The hydrogen positions were included in the refinement for four cycles of full-matrix least-squares refinement and thereafter held fixed. The model converged with $R = 3.5\%$, $R_w = 3.6\%$. The error in an observation of unit weight is 1.57. A structure factor calculation with all observed and unobserved reflections included (no refinement) gave $R = 4.0\%$; on this basis it was decided that careful measurement of reflections rejected automatically during data collection would not significantly improve the results. A final Fourier difference map was featureless. A table of the observed structure factors is available.[27] *Mass spectra* were obtained using a Perkin Elmer RMU-6E mass spectrometer.

RESULTS AND DISCUSSION

Final positional and thermal parameters for the complex FeM · Nbz are given in Table I. Tables II and III contain the bond lengths and angles. The digits in parentheses in the tables are the estimated standard deviations in the last significant figures quoted and were derived from the inverse matrix in the course of least squares refinement calculations. Figure 3 is a stereoscopic pair view of the complex, and Fig. 4 shows the molecular packing in the unit cell. Table IV gives the nearest intermolecular contacts, and Table V the closest approaches to the included nitrobenzene molecule. It is evident that the nitrobenzene molecule is well isolated from the complex molecules which are well isolated from each other. FeM · Nbz is pure low spin ($^2T_2$ split mainly by trigonal but also some tetragonal distortion as evidenced by the crystal structure) in the region 0–100 K,[11] rather like FeM · $(C_6H_6)_2$.[9] Thus, benzene and

TABLE I. Positional and thermal parameters and their estimated standard deviations for FeM·Nbz.

Atom	*X*	*Y*	*Z*	*B*(1,1)	*B*(2,2)	*B*(3,3)	*B*(1,2)	*B*(1,3)	*B*(2,3)
FE	0.23160(7)	0.11845(2)	0.21809(6)	0.00904(6)	0.000710(6)	0.00858(6)	0.00021(4)	0.0048(1)	0.00041(4)
S(11)	0.2524(1)	0.17047(4)	0.3940(1)	0.0094(1)	0.00094(1)	0.0123(1)	−0.00110(7)	0.0055(2)	−0.00168(7)
S(12)	−0.0033(1)	0.13063(4)	0.2361(1)	0.0102(1)	0.00092(1)	0.0114(1)	−0.00102(7)	0.0055(2)	−0.00185(7)
S(21)	0.3026(1)	0.06262(3)	0.3832(1)	0.0127(2)	0.00093(1)	0.0071(1)	−0.00058(8)	0.0017(2)	−0.00015(7)
S(22)	0.1735(1)	0.05499(4)	0.0857(1)	0.0119(1)	0.00107(1)	0.0070(1)	0.00077(8)	0.0020(2)	0.00063(7)
S(31)	0.4649(1)	0.12945(4)	0.1934(1)	0.0099(1)	0.00104(1)	0.0129(1)	0.00141(8)	0.0048(2)	0.00271(7)
S(32)	0.2050(1)	0.16398(4)	0.0225(1)	0.0091(1)	0.00106(1)	0.0125(1)	0.00123(7)	0.0055(2)	0.00245(7)
O(1)	−0.1433(4)	0.22779(11)	0.6235(3)	0.0168(5)	0.00157(5)	0.0172(4)	0.0007(3)	0.0172(7)	−0.0023(2)
O(2)	0.2673(4)	−0.10310(9)	0.2769(3)	0.0240(6)	0.00081(3)	0.0142(4)	0.0021(3)	−0.0014(9)	−0.0006(2)
O(3)	0.6049(3)	0.22736(11)	−0.1940(3)	0.0146(4)	0.00155(5)	0.0175(4)	−0.0017(2)	0.0141(7)	0.0019(2)
O(1B)	0.1045(4)	0.39439(12)	0.1153(4)	0.0293(7)	0.00146(5)	0.0305(6)	−0.0034(3)	0.0265(11)	−0.0021(3)
O(2B)	0.3295(5)	0.38683(13)	0.2447(4)	0.0335(7)	0.00190(5)	0.0263(6)	0.0080(3)	0.0255(10)	0.0038(3)
N(1)	−0.0042(3)	0.1914(1)	0.4317(3)	0.0101(4)	0.00090(4)	0.0104(4)	0.0000(2)	0.0067(7)	−0.0014(2)
N(2)	0.2515(4)	−0.0137(1)	0.2535(3)	0.0102(4)	0.00079(4)	0.0073(4)	−0.0005(2)	−0.0002(7)	0.0000(2)
N(3)	0.4595(3)	0.1864(1)	−0.0140(3)	0.0087(4)	0.00115(4)	0.0130(4)	0.0009(2)	0.0072(7)	0.0029(2)
N(1B)	0.2235(5)	0.4085(1)	0.2088(4)	0.0227(6)	0.00151(6)	0.0151(5)	0.0008(4)	0.0203(8)	0.0007(3)
C(11)	0.0710(4)	0.1675(1)	0.3648(4)	0.0098(5)	0.00064(4)	0.0097(5)	−0.0008(3)	0.0055(8)	0.0004(2)
C(21)	0.2430(4)	0.0286(1)	0.2424(4)	0.0076(5)	0.00081(4)	0.0081(5)	−0.0001(3)	0.0027(8)	0.0005(2)
C(31)	0.3867(4)	0.1632(1)	0.0548(4)	0.0091(5)	0.00078(5)	0.0102(5)	0.0007(3)	0.0055(8)	0.0007(3)
C(12)	−0.1608(5)	0.1901(2)	0.4032(5)	0.0112(6)	0.00124(6)	0.0161(6)	−0.0003(3)	0.0086(10)	−0.0019(3)
C(13)	−0.2042(5)	0.1926(2)	0.5380(5)	0.0147(6)	0.00136(7)	0.0226(7)	−0.0009(4)	0.0213(11)	−0.0010(4)
C(14)	0.0626(5)	0.2256(1)	0.5295(5)	0.0136(6)	0.00120(6)	0.0161(6)	−0.0015(3)	0.0098(11)	−0.0040(3)
C(15)	0.0058(6)	0.2255(2)	0.6590(5)	0.0194(8)	0.00163(7)	0.0143(6)	0.0013(4)	0.0072(12)	−0.0027(4)
C(22)	0.3320(5)	−0.0343(1)	0.3856(4)	0.0157(7)	0.00097(5)	0.0097(5)	0.0004(3)	−0.0008(11)	0.0010(3)
C(23)	0.2883(6)	−0.0782(1)	0.3990(5)	0.0226(9)	0.00094(6)	0.0136(6)	0.0004(4)	−0.0046(14)	0.0007(3)
C(24)	0.2105(5)	−0.0410(1)	0.1274(4)	0.0157(7)	0.00120(6)	0.0093(5)	−0.0002(4)	−0.0014(11)	−0.0007(3)
C(25)	0.1721(6)	−0.0841(1)	0.1609(5)	0.0235(9)	0.00077(5)	0.0150(7)	0.0001(4)	−0.0043(13)	−0.0019(3)
C(32)	0.3907(5)	0.2188(2)	−0.1175(5)	0.0124(7)	0.00179(7)	0.0200(7)	0.0011(4)	0.0080(12)	0.0077(3)
C(33)	0.4558(6)	0.2229(2)	−0.2351(5)	0.0213(9)	0.00197(8)	0.0177(7)	−0.0010(5)	0.0108(13)	0.0049(4)
C(34)	0.6165(5)	0.1885(2)	0.0212(5)	0.0125(7)	0.00153(7)	0.0192(7)	0.0010(4)	0.0096(12)	0.0032(4)
C(35)	0.6674(5)	0.1929(2)	−0.1073(6)	0.0140(7)	0.00161(7)	0.0228(8)	0.0010(4)	0.0185(11)	0.0012(4)
C(1B)	0.2367(5)	0.4551(1)	0.2286(4)	0.0143(6)	0.00107(5)	0.0098(5)	0.0002(4)	0.0116(8)	0.0005(3)
C(2B)	0.3678(5)	0.4723(2)	0.2957(5)	0.0116(6)	0.00192(8)	0.0136(6)	0.0025(4)	0.0091(10)	0.0018(4)
C(3B)	0.3808(5)	0.5154(2)	0.3114(5)	0.0127(7)	0.00216(8)	0.0136(6)	−0.0031(4)	0.0073(11)	−0.0016(4)
C(4B)	0.2638(5)	0.5410(2)	0.2639(5)	0.0172(7)	0.00139(6)	0.0153(6)	−0.0028(4)	0.0130(11)	−0.0018(3)
C(5B)	0.1350(5)	0.5236(2)	0.1991(5)	0.0144(7)	0.00129(6)	0.0156(6)	0.0011(4)	0.0098(11)	0.0003(3)
C(6B)	0.1203(5)	0.4804(2)	0.1794(4)	0.0106(6)	0.00132(6)	0.0131(6)	−0.0011(3)	0.0054(10)	−0.0001(3)
H(121)	−0.204(5)	0.215(1)	0.339(4)	6.(1)					
H(122)	−0.191(4)	0.164(1)	0.350(4)	5.(1)					
H(131)	−0.167(4)	0.166(1)	0.591(4)	6.(1)					
H(132)	−0.308(4)	0.193(1)	0.517(4)	6.(1)					
H(141)	0.158(4)	0.221(1)	0.559(4)	5.(1)					
H(142)	0.035(5)	0.255(1)	0.482(5)	8.(1)					
H(151)	0.049(5)	0.251(1)	0.719(4)	6.(1)					
H(152)	0.042(5)	0.198(1)	0.713(4)	7.(1)					
H(221)	0.434(5)	−0.035(1)	0.382(4)	6.(1)					
H(222)	0.324(4)	−0.017(1)	0.465(4)	5.(1)					
H(231)	0.194(5)	−0.077(1)	0.422(4)	8.(1)					
H(232)	0.360(4)	−0.092(1)	0.473(4)	4.(1)					
H(241)	0.137(4)	−0.028(1)	0.065(4)	4.(1)					
H(242)	0.299(5)	−0.042(1)	0.084(4)	7.(1)					
H(251)	0.171(4)	−0.101(1)	0.078(4)	6.(1)					
H(252)	0.077(5)	−0.083(1)	0.179(4)	7.(1)					
H(321)	0.292(5)	0.212(1)	−0.154(4)	7.(1)					
H(322)	0.408(5)	0.248(1)	−0.072(5)	8.(1)					
H(331)	0.420(5)	0.250(1)	−0.290(4)	6.(1)					
H(332)	0.432(5)	0.195(2)	−0.290(5)	9.(1)					
H(341)	0.650(4)	0.214(1)	0.084(4)	8.(1)					
H(342)	0.654(4)	0.160(1)	0.068(4)	6.(1)					
H(351)	0.634(5)	0.614(1)	−0.160(4)	8.(1)					
H(352)	0.767(4)	0.196(1)	−0.083(4)	6.(1)					
H(2B)	0.441(4)	0.453(1)	0.330(4)	6.(1)					
H(3B)	0.473(5)	0.528(1)	0.352(4)	6.(1)					
H(1B)	0.276(4)	0.573(1)	0.277(4)	6.(1)					
H(5B)	0.054(4)	0.540(1)	0.165(4)	6.(1)					
H(6B)	0.033(4)	0.468(1)	0.139(4)	5.(1)					

The form of the anisotropic thermal parameter is $\exp[-B(1,1)*H*H+B(2,2)*K*K+B(3,3)*L*L+B(1,2)*H*K+B(1,3)*H*L+B(2,3)*K*L)]$.

nitrobenzene act similarly. The magnetism of FeM·Mbz is in sharp contrast with that of the unsolvated complex FeM, which shows a rapid rise in μ over this temperature range from essentially low spin to largely high spin values in this region. The properties of FeM·Nbz contrast even more with those of FeM·CH_2Cl_2 and FeM·$CHCl_3$ for which magnitudes of the low temperature magnetic moments are appropriate to $S=\frac{3}{2}$ ground states leading to the postulates of the first such ground states in *tris*(dithiocarbamates). In keeping with their similar magnetic properties the average iron–sulfur bond lengths ⟨Fe–S⟩ of FeM·$(C_6H_6)_2$ and FeM·Nbz are approximately the same.

It is now clear that the solvent molecules included in the lattice have specific effects on the structure and

TABLE II. Bond distances (Å) for FeM · Nbz.

Fe–S(11)	2.336(1)	C(12)–C(13)	1.478(5)
Fe–S(12)	2.365(1)	C(13)–O(1)	1.417(4)
Fe–S(21)	2.356(1)	O(1)–C(15)	1.401(5)
Fe–S(22)	2.360(1)	C(14)–C(15)	1.500(5)
Fe–S(31)	2.365(1)	C(22)–C(23)	1.461(4)
Fe–S(32)	2.339(1)	C(23)–O(2)	1.391(4)
S(11)–C(11)	1.713(3)	O(2)–C(25)	1.393(4)
S(12)–C(11)	1.721(3)	C(24)–C(25)	1.463(5)
S(21)–C(21)	1.715(3)	C(32)–C(33)	1.448(5)
S(22)–C(21)	1.712(3)	C(33)–O(3)	1.406(5)
S(31)–C(31)	1.728(5)	O(3)–C(35)	1.409(5)
S(32)–C(31)	1.711(3)	C(34)–C(35)	1.464(5)
C(11)–N(1)	1.328(4)	C(1B)–C(2B)	1.381(5)
C(21)–N(2)	1.333(3)	C(1B)–C(6B)	1.364(5)
C(31)–N(3)	1.313(4)	C(2B)–C(3B)	1.365(5)
N(1)–C(12)	1.474(4)	C(3B)–C(4B)	1.373(5)
N(1)–C(14)	1.470(4)	C(4B)–C(5B)	1.362(5)
N(2)–C(22)	1.468(3)	C(5B)–C(6B)	1.372(5)
N(2)–C(24)	1.464(4)	C(1B)–N(1B)	1.477(5)
N(3)–C(32)	1.465(4)	N(1B)–O(1B)	1.221(4)
N(3)–C(34)	1.475(4)	N(1B)–O(2B)	1.207(4)

TABLE III. Bond angles (in deg) for FeM · Nbz.

S(11)–Fe–S(12)	74.60(3)	S(22)–C(21)–N(2)	123.9(2)
S(11)–Fe–S(21)	93.91(3)	S(31)–C(31)–S(32)	112.1(2)
S(11)–Fe–S(22)	162.37(4)	S(31)–C(31)–N(3)	123.5(2)
S(11)–Fe–S(31)	93.95(4)	S(32)–C(31)–N(3)	124.4(2)
S(11)–Fe–S(32)	97.89(3)	C(11)–N(1)–C(12)	124.4(3)
S(12)–Fe–S(21)	100.82(4)	C(11)–N(1)–C(14)	121.5(3)
S(12)–Fe–S(22)	94.49(3)	C(12)–N(1)–C(14)	113.7(3)
S(12)–Fe–S(31)	162.22(3)	C(21)–N(2)–C(22)	121.1(2)
S(12)–Fe–S(32)	93.20(3)	C(21)–N(2)–C(24)	121.3(2)
S(21)–Fe–S(22)	74.26(3)	C(22)–N(2)–C(24)	116.2(3)
S(21)–Fe–S(31)	93.38(3)	C(31)–N(3)–C(32)	121.7(3)
S(21)–Fe–S(32)	163.67(4)	C(31)–N(3)–C(34)	124.6(3)
S(22)–Fe–S(31)	99.66(4)	C(32)–N(3)–C(34)	112.8(3)
S(22)–Fe–S(32)	96.50(3)	N(1)–C(12)–C(13)	110.4(3)
S(31)–Fe–S(32)	74.64(3)	C(12)–C(13)–O(1)	112.9(3)
Fe–S(11)–C(11)	87.2(1)	C(13)–O(1)–C(15)	110.6(3)
Fe–S(12)–C(11)	86.1(1)	O(1)–C(15)–C(14)	112.0(3)
Fe–S(21)–C(21)	86.7(1)	C(15)–C(14)–N(1)	110.2(3)
Fe–S(22)–C(21)	86.7(1)	N(2)–C(22)–C(23)	113.1(3)
Fe–S(31)–C(31)	86.0(1)	C(22)–C(23)–O(2)	115.9(3)
Fe–S(32)–C(31)	87.2(1)	C(23)–O(2)–C(25)	111.7(3)
S(11)–C(11)–S(12)	112.1(2)	O(2)–C(25)–C(24)	115.0(3)
S(11)–C(11)–N(1)	124.2(2)	C(25)–C(24)–N(2)	112.7(3)
S(12)–C(11)–N(1)	123.7(2)	N(3)–C(32)–C(33)	112.9(3)
S(21)–C(21)–S(22)	112.4(2)	C(32)–C(33)–O(3)	114.4(4)
S(21)–C(21)–N(2)	123.8(2)	C(33)–O(3)–C(35)	110.2(3)
O(3)–C(35)–C(34)	113.1(3)	C(2B)–C(1B)–C(6B)	121.1(3)
C(35)–C(34)–N(3)	111.4(3)	C(1B)–C(2B)–C(3B)	119.2(4)
O(1B)–N(1B)–O(2B)	124.1(4)	C(2B)–C(3B)–C(4B)	120.1(4)
O(1B)–N(1B)–C(1B)	117.1(4)	C(3B)–C(4B)–C(5B)	120.0(4)
O(2B)–N(1B)–C(1B)	118.9(5)	C(4B)–C(5B)–C(6B)	120.8(4)
N(1B)–C(1B)–C(2B)	119.1(4)	C(5B)–C(6B)–C(1B)	118.8(3)
N(1B)–C(1B)–C(6B)	119.8(4)		

magnetisms of the complexes. Solvents capable of hydrogen bonding, such as $CHCl_3$, CH_2Cl_2, and H_2O, shift the high spin–low spin equilibrium towards the high spin side, and may give rise to intermediate spin states which are not observed in the unsolvated complexes. In the cases structurally investigated by x-ray methods hydrogen-bonding interactions with ligand sulfur atoms were observed, and these are the probable cause of the magnetic effect. The hydrogen bonding interaction with a sulfur atom must weaken the Fe–S bond slightly, thereby weakening the crystal field splitting (Δ) significantly [$\Delta \sim (\langle Fe-S \rangle)^{-5}$]. This in turn would lengthen all the Fe–S bonds, amplifying the original effect.

The effect of included molecules which are not capable of hydrogen bonding is equally dramatic on both the magnetism and the structure, but is more surprising since no direct contacts are apparant in any of the three (precise) structure determinations carried out: FeP · $(C_6H_6)_2$,[14] FeM · $(C_6H_6)_2$,[9] and FeM · Nbz (this work). The interaction of benzene and nitrobenzene with the complex molecules could be dipolar, and at-

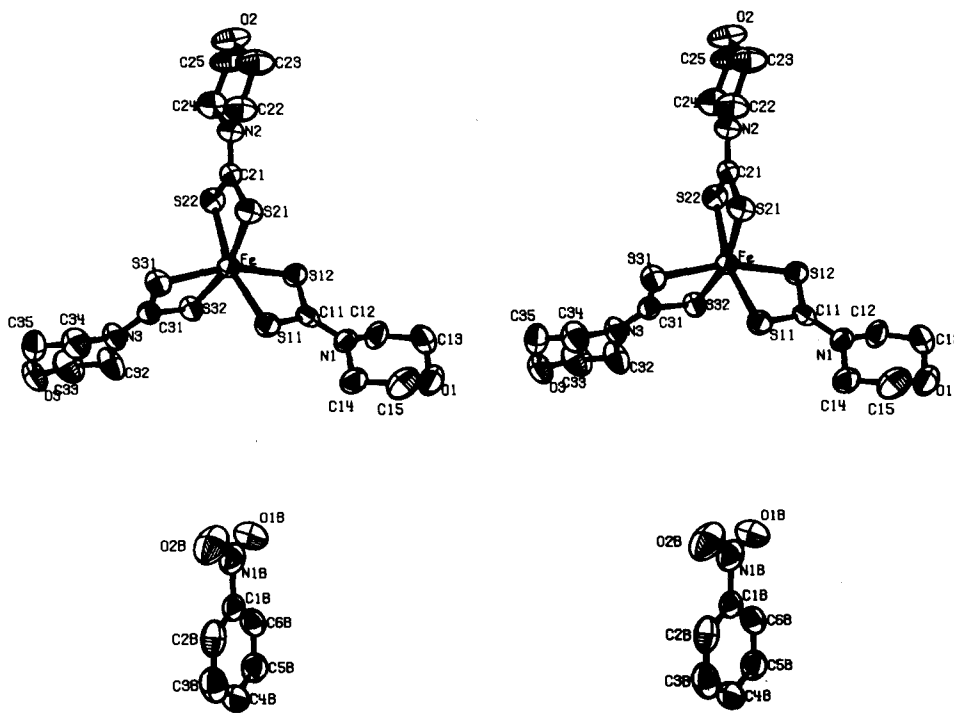

FIG. 3. Stereopair view of FeM · Nbz.

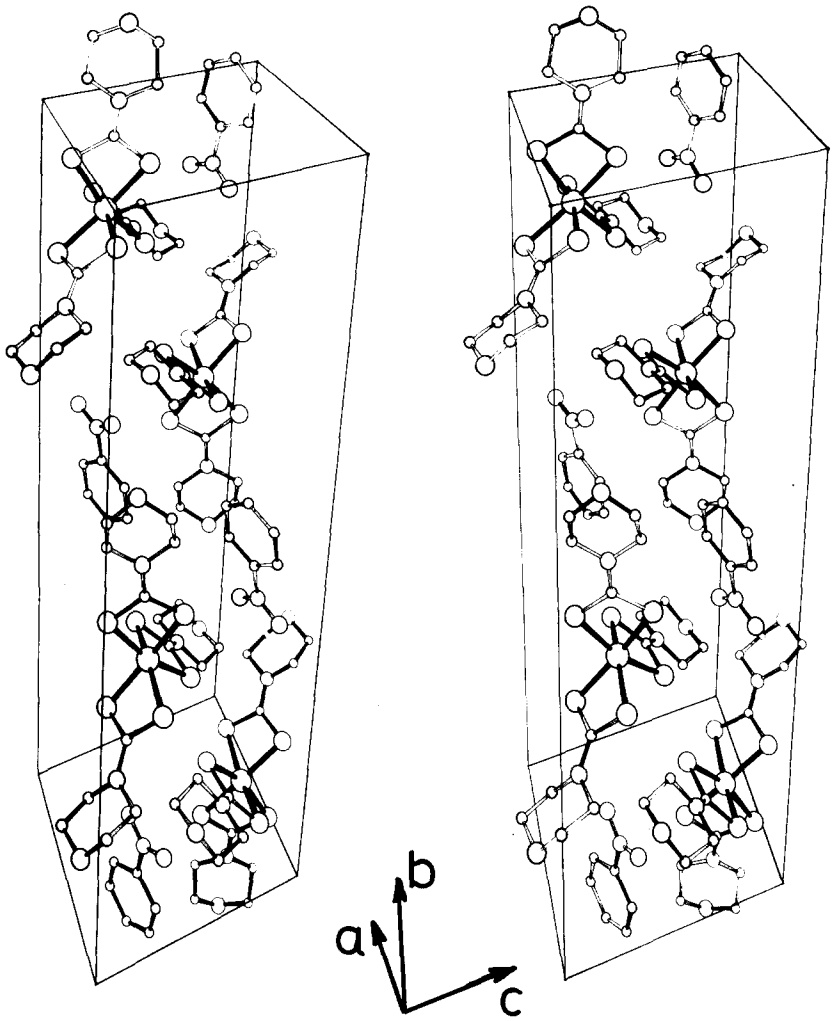

FIG. 4. Molecular packing in FeM • Nbz.

tempts will be made to verify this if it is possible to include molecules for which such dipolar effects would be much higher or much lower than nitrobenzene or benzene. On the other hand, it is possible that the included solvent molecules merely act as diluents for some kind of cooperative interaction between neighboring complex molecules, which tends to favor high spin ground states in the unsolvated complexes. Then the shift towards the low spin side of the equilibrium would arise from the absence of the interactions when intervening benzene or nitrobenzene separates the complex molecules.

The most dramatic demonstration of the solvent effect is in FeP• $(C_6H_6)_{1/2}$, which lies at the high spin–low spin crossover, consisting almost entirely of high spin species at room temperature, and essentially pure low spin species at liquid helium temperature. It is the only dithiocarbamate complex for which so complete a transformation of spin states has been observed with temperature variation alone. By contrast, the unsolvated complex and the chloroform solvate (unstable with respect to loss of chloroform, *vide supra*) are purely high spin. Thus, the presence or absence of a solvent molecule in the lattice, but not in close contact with the FeP molecule, determines whether the complex is high spin or not. Insertion of benzene into the lattice therefore changes not only the magnitude of the susceptibility (χ) and moments (μ), but also drastically changes the char-

TABLE IV. Closest intermolecular contancts (Å) for FeM • Nbz.

Molecule 1	Molecule 2	Distance	Symmetry transformation		
O(1)	O(3)	3.373	$x-1$	y	$1+z$
	C(34)	3.484	$x-1$	$\frac{1}{2}-y$	$\frac{1}{2}+z$
	C(35)	3.533	$x-1$	$\frac{1}{2}-y$	$\frac{1}{2}+z$
O(2)	C(35)	3.408	$1-x$	$-y$	$-z$
	C(13)	3.477	$1-x$	$-y$	$-z$
O(3)	C(12)	3.416	$1+x$	$\frac{1}{2}-y$	$z-\frac{1}{2}$
	C(13)	3.561	$1+x$	$\frac{1}{2}-y$	$z-\frac{1}{2}$

TABLE V. Contacts with included solvent (Å) for FeM • Nbz.

Molecule 1	Molecule 2	Distance	Symmetry transformation		
O(1B)	C(11)	3.373	x	$\frac{1}{2}-y$	$z-\frac{1}{2}$
	N(1)	3.450	x	$\frac{1}{2}-y$	$z-\frac{1}{2}$
O(2B)	N(3)	3.294	x	$\frac{1}{2}-y$	$z-\frac{1}{2}$
	C(31)	3.316	x	$\frac{1}{2}-y$	$z-\frac{1}{2}$
	C(32)	3.570	x	$\frac{1}{2}-y$	$z-\frac{1}{2}$
N(1B)	S(21)	3.562	x	$\frac{1}{2}-y$	$z-\frac{1}{2}$

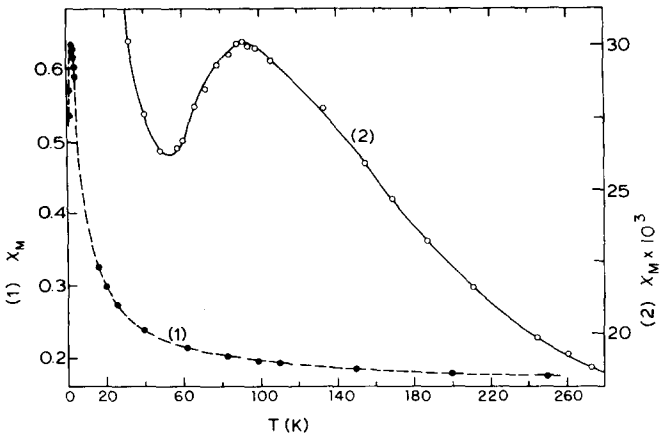

FIG. 5. Temperature dependence of the molar magnetic susceptibility, χ_M (cgs emu) for FeP (●, scale 1), and for FeP·$(C_6H_6)_{1/2}$ (○, scale 2). Two scales are required because the susceptibility of FeP is much higher than that of FeP·$(C_6H_6)_{1/2}$ at each point.

acter of the χ versus T curve, as shown in Fig. 5. However, this result is not too surprising in view of earlier indications that FeP does lie close to the high spin–low spin crossover; in chloroform solution the spin state equilibrium is observed at high pressures, the equilibrium being shifted in favor of the low spin species with increasing pressures.[2] It now seems likely that the conclusion of Golding and Whitfield[28] that the $^6A_1$ state lies at least 2000 cm^{-1} below the $^2T_2$ state in FeP constitutes an overestimate. Figure 6 shows the depression of μ versus T curve for FeP when benzene is included in the lattice, together with the analogous results for $FeBu_2$. The unsolvated di-*n*-butyl complex $FeBu_2$ exhibits the spin state equilibrium,[2] and the equilibrium is shifted towards the low spin side when benzene is included in the lattice, in keeping with the observation that ⟨Fe–S⟩ is shorter in the benzene solvate (2.341 Å)[12] than in the unsolvated complex (2.42 Å).[29] This agrees well with a similar shift in the equilibrium and shortening of ⟨Fe–S⟩ [2.430 Å in FeM·CH_2Cl_2 to 2.318 Å in FeM·$(C_6H_6)_2$[9]], and the effect is therefore general. The data on FeP, FeM, and $FeBu_2$ together indicate that the FeS_6 core is extremely sensitive to distortion. The inclusion of various solvent molecules in the lattice can produce as marked an effect on the spin state equilibrium and the ⟨Fe–S⟩ distance as a temperature change of several hundred degrees, a pressure change of several thousand atmospheres, or a chemical modification of the ligand itself. The effect is greater, as well as more surprising, for solvents such as benzene and nitrobenzene, which do not interact with the complex molecules, than for such solvents as chloroform, dichloromethane, or water, which can take part in hydrogen bonding interactions.

The high spin form of FeP has a maximum in the χ versus T curve near 2 K (Fig. 5), which is inconsistent with its known spin state,[2,4,30] even if zero field splitting[30] is taken into account. To check on antiferromagnetic interactions the magnetic properties were examined in the liquid helium region, diluted in various concentrations in the diamagnetic CoP complex and in frozen chloroform solution. The interpretation of the magnetism of FeP in various concentrations in the CoP host now has an additional complicating factor. Like benzene CoP is not in close contact with the FeP molecules and therefore a similar mechanism as that observed in benzene solvates might be postulated *a priori*. However, the effect of adding CoP to the lattice is initially the same as that of adding benzene: When a small amount of CoP is added to the FeP lattice the susceptibility of the overall diluted sample is greater than that of the pure FeP, despite the dilution. Therefore, the contribution of the FeP to the susceptibility of the diluted sample is much greater than that of pure FeP. At high dilutions, especially when the CoP concentration rises above 50%, the moment of FeP begins to decrease again. However, this is considered to arise because the FeP molecule distorts slightly (*vide infra*) to approach that of the CoP host lattice rather than from the mechanism acting in FeM·$(C_6H_6)_{1/2}$. The χ versus T curves for various (higher) concentrations of FeP in CoP are shown in Fig. 7. Each point on the curve is an independent determination, measured from the flux change when the sample is put into the field (115 Oe), independent of any external calibration constant which must be used in other methods. Each determination has higher accuracy than the relative values obtained from most other techniques. The data agree within experimental error with the measurements made on a Foner balance using a wide range of magnetic fields. Thus, the susceptibility anomaly is in no way due to saturation effects.

The susceptibility anomaly gradually disappears upon increasing dilution with the cobalt complex, and the magnetism tends towards Curie law behavior at high dilution, both in frozen chloroform solution and in the cobalt complex. (The frozen chloroform solution data are of lower accuracy because of the much higher dilution and uncertainty of even distribution of the FeP in the presumed $CHCl_3$ glasses.) The μ_{Fe} versus T curves rise steadily towards the high spin limit as shown in Fig. 8. The behavior of the dilute samples demonstrates the absence of a high spin–low spin equilibrium

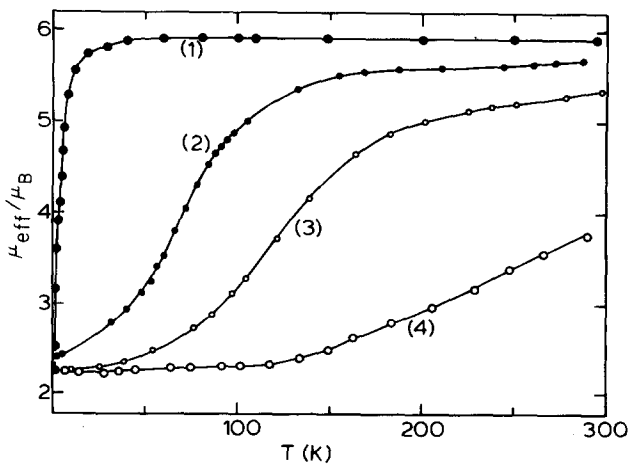

FIG. 6. Temperature dependence of effective magnetic moments of (1) FeP, (2) FeP·$(C_6H_6)_{1/2}$, (3) $FeBu_2$, (4) $FeBu_2$·(C_6H_6).

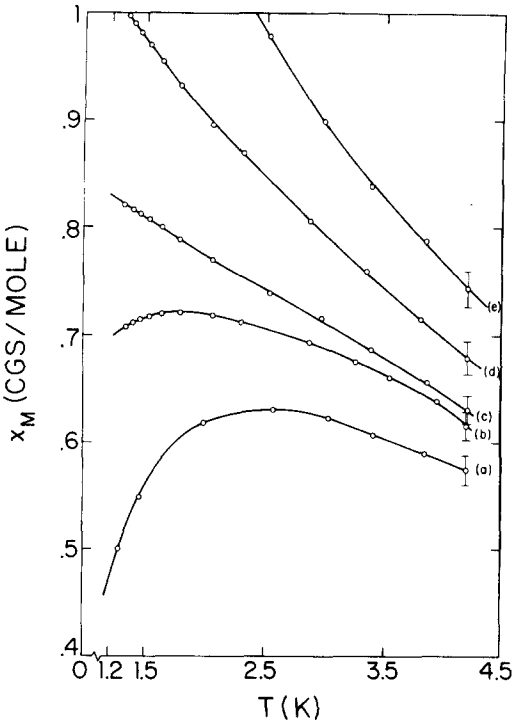

FIG. 7. Magnetic susceptibilities as a function of temperature, for the proportions in Fig. 8, of FeP in CoP.

in the complex. It is possible to attain a measurable population of the low spin state in liquid solution at high pressure,[2] but in the solid or frozen solution the complex is purely high spin.

The effect of dilution in FeP can only be explained by antiferromagnetic interactions, gradually broken up upon increasing dilution by separation of the magnetic species. The x-ray crystal structural determination[31] of FeP shows that the complex consists of isolated molecules, with only van der Waals contacts between ligand atoms of neighboring molecules. From the structural data we obtain the nearest Fe–Fe distance as 8.7 Å, and the nearest intermolecular approaches of ligand sulfur atoms as 4.9 Å, too large to produce antiferromagnetic interactions of the magnitude required (~2 cm^{-1}) to account for the susceptibility maximum in pure FeP complex. It is unlikely that direct dipole interactions over such distances will be detectable in our experiments. However, proton NMR spectra show large electron spin delocalization on to the ligand protons,[32] implying successively much larger delocalization on to the ligand atoms closer to the metal atoms. The intermolecular approach of the various ligand atoms is much closer than the 9 Å Fe–Fe distance, thereby providing a mechanism for far greater antiferromagnetic interaction.

In marked contrast to the iron(III) complex, CrP shows no susceptibility anomaly. The moment drops relatively little with decreasing temperature, and a dilution experiment, analogous to the one described above, indicates a significant but much smaller antiferromagnetic interaction. The proton NMR peaks show considerable paramagnetic broadening, but smaller shifts than in the iron(III) complex.[33] Thus, there is less unpaired spin delocalization on to the ligand protons in CrP, implying relatively less delocalization on to the other ligand atoms. Thus, the spin delocalization mechanism for antiferromagnetism is expected to be less effective in the Cr complex, and indeed the complex exhibits much less antiferromagnetism than FeP. The main difference between the ground states of the ferric ($^6A_1$, $t_2^3e^2$) and chromium ($^4T_2$, t_2^3) complexes are two electrons in the e orbitals (d_{z2} and $d_{x^2-y^2}$) possessed by the iron and not by the chromium. Thus, these electrons are likely to be responsible for much or most of the delocalization effects as well as the antiferromagnetic interactions. Of course, low-lying excited states may exert some influence on the iron(III) ground state, but there is no evidence, especially from the present magnetic data, that the $^2T_2$ (t_2^5) or the $^4T_1$ (t_2^4e) are close enough to be more than of minor importance.

The Mössbauer spectra, in both isolated[34] (dilute) and concentrated[4,35] FeP molecules, and the infrared magnetic resonance data, are best explained in terms of a negative zero-field splitting D, such that $|M_s=\pm\frac{5}{2}\rangle$ lie lowest, where D is defined by the Hamiltonian

$$\mathcal{H}=D[S_z^2-\tfrac{1}{3}S(S+1)]+g\beta\mathbf{H}\cdot\mathbf{S}\,. \tag{1}$$

Thus, at low temperatures the system is "locked into" the $|\pm\frac{5}{2}\rangle$ states, thereby producing a residual intramolecular magnetic field because transitions between $|\frac{5}{2}\rangle$ and $|-\frac{5}{2}\rangle$ are forbidden and relaxation via the $|M_s=\pm\frac{3}{2}, \pm\frac{1}{2}\rangle$ states is thermally prohibited. A D value of -2.14 (± 0.05) cm^{-1}, estimated from the infrared absorption, is compatible with the Mössbauer data (as indicated by the appearance of peak splitting, when the residual intramolecular field is unaveraged on the Mössbauer time

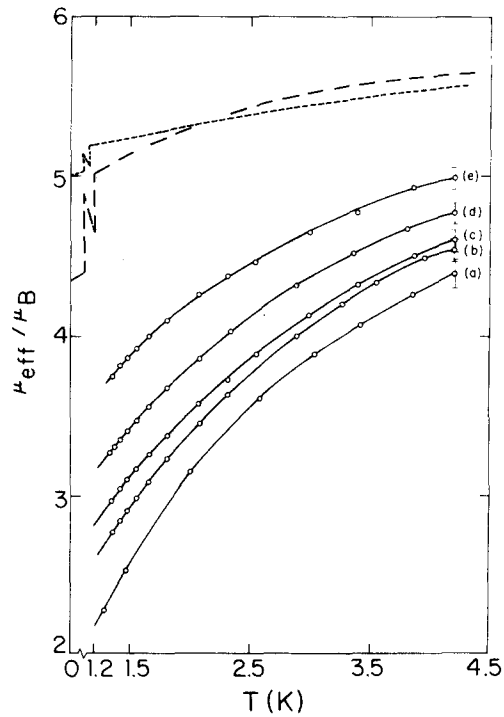

FIG. 8. Magnetic moments as a function of temperature for several concentrations of FeP in CoP. Curve (a) is for 100% FeP, (b) 88%, (c) 86%, (d) 67%, (e) 61%. The theoretical curves for infinite dilution, with a zero-field splitting D of -2.14 (-----) and $+2.14$ (— —) are also shown.

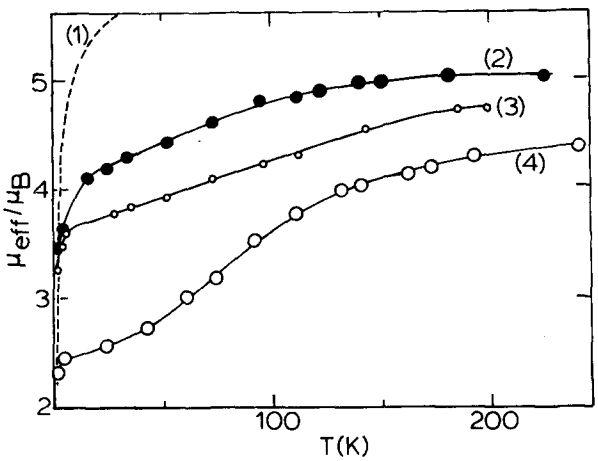

FIG. 9. Magnetic moments as a function of temperature, for several concentrations of FeP in CoP: (1) 100%, (2) 33%, (3) 20%, (4) 5%.

scale). However, it is clear that the system is not as simple as this model would indicate, since the antiferromagnetism is not taken into account, but it is of interest to examine the dilute FeP, from which the magnetic interaction has been removed.

For a $^6A_1$ system the magnetic interaction is described by the Hamiltonian (1) and the susceptibility defined by

$$\chi_M = -\frac{N}{H}\left(\sum_i \frac{\partial E_i}{\partial H} e^{-E_i/kT}\right)\Big/\left(\sum_i e^{-E_i/kT}\right) ,$$

where, for a powder, both the perpendicular and parallel directions must be considered. Using $D \gg \beta H$ to evaluate E_i from (1) with perturbation theory (this is satisfied for all measurable values of D, since $\beta H = 0.0054$ cm^{-1} in these experiments), we have

$$\mu_{eff}^2 = \frac{19x + 16 + (9x - 11)y + (25x - 5)y^3}{(1 + y + y^3)x} , \qquad (2)$$

where $D = xkT$ and $y = e^{-x}$. For $D \to 0$, $\mu_{eff} \to \sqrt{19}$ BM (D positive) or 5 BM (D negative). The μ_{eff} versus T curves for FeP do tend towards Eq. (2) (Fig. 8), with $D = -2.14$ cm^{-1} (the curve for $D = +2.14$ cm^{-1} is also shown) as they progress towards higher dilution, but the limit of infinite dilution cannot be studied for the high spin form because the moments increase again at high dilution, indicating a change of spin state.

At high dilution with CoP the moment of FeP becomes temperature dependent and lies consistently below the high spin limit. This suggests that the structure of the FeP molecule is modified slightly (presumably with a shortening of the Fe–S bond lengths) to approach those of the CoP host lattice, which has shorter metal–sulfur bonds. The temperature dependence of the moments (Fig. 9) at various high dilution is much less (and the χ versus T curves show no maxima or minima) than in a pure crossover system such as FeP · $(C_6H_6)_{1/2}$. This suggests that the FeP is less free to change its metal–sulfur bond lengths in the CoP host lattice. The smaller antiferromagnetic interactions in CrP have been investigated less extensively than those in FeP, but the 69% sample [curve (b) in Fig. 10] can be used to estimate the upper limit for D. If Eq. (1) is assumed to give the only deviation of the moment from the high spin value of $\sqrt{15}$ BM for $^4A_2$, then μ_{eff} is given by Eq. (3), which has the same value whether D is positive or negative:

$$\mu_{eff}^2 = 9 + \frac{6(1 - y)}{x(1 + y)} . \qquad (3)$$

Curve (b) of Fig. 10 now gives $|D| < 1.2$ cm^{-1}.

The properties of the diluent CoP, used in these experiments, are optimal; it was found to have negligible susceptibility. This agrees with theoretical expectations; the temperature independent paramagnetism of 300×10^{-6} cgs, calculated as described previously[36] using optical spectra and ^{59}Co NMR data[37,38] to obtain $k = 0.75$ for the orbital reduction factor,[39] approximately cancels the molecular diamagnetism of -280×10^{-6} cgs.

Given better understanding of the FeP system now possible, it would be expected that ⟨Fe–S⟩ would be greater in the pure high spin FeP than in FeP · $(C_6H_6)_{1/2}$. The reverse is the case, suggesting that the less accurate x-ray structure determination (FeP),[31] which does not fit well into the series of known iron(III) dithiochelate complexes (Table VI), underestimates ⟨Fe–S⟩. This would not be surprising, as that work was fraught with experimental difficulties mainly due to crystal quality. At least for analogous compounds [such as the FeM series, the $FeBu_2$ series, $FeEt_2$, and probably the pair FeP and FeP · $(C_6H_6)_{1/2}$] there is a general correlation between magnetic moment and ⟨Fe–S⟩.

CONCLUSION

The inclusion of benzene and nitrobenzene in the dithiocarbamate crystal lattice shifts existing high spin

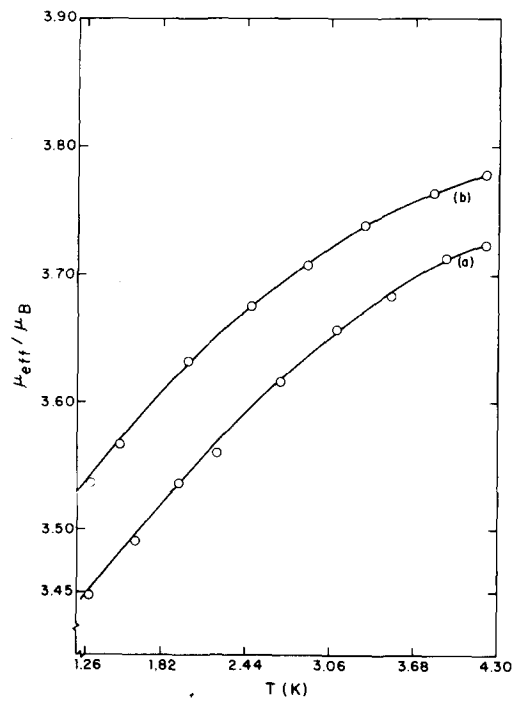

FIG. 10. Magnetic susceptibilities as a function of temperature for (a) 100% CrP and (b) 68.6% CrP in CoP.

TABLE VI. Magnetic and structural features of some ferric dithiochelates.

	μ (D)	⟨Fe–S⟩ (Å)	ϕ[a]	⟨S–Fe–S⟩ (deg)	Reference
$FeEt_2$ (79 K)	2.2	2.306	40.5	75.9	7
$Fe[S_2C-S-C(CH_3)_3]_3$	2.5	2.297	42.0	75.2	39, 40
$Fe(S_2CO-Et)_3$	2.7	2.316	41.2	75.5	41
$Fe[S_2CN(CH_3)\cdot C_6H_5]_3$	2.9	2.312	40.4	75.1	31
$FeM\cdot(C_6H_6)_2$	3.5	2.318	42.5	75.5	9
$FeBu_2\cdot(C_6H_6)$	3.6	2.341	40.2	74.6	12
$FeEt_2$ (297 K)	4.3	2.357	37.6	74.3	7
$FeM\cdot CHCl_3$	5.5	2.416	33.8	73.3	9
$FeM\cdot CH_2Cl_2$	5.1	2.430	33.6	72.6	8
$FeBu_2$	5.3	2.42	33.2	72.8	29
$FeP\cdot(C_6H_6)_{1/2}$	5.6	2.434	37.1	73.3	14
$FeM\cdot H_2O$	5.6	2.443	31.5	72.7	9
FeP	5.9	2.41	38.6	74.5	31

[a]Trigonal twist angle, as defined in Ref. 11.

⇄low spin equilibria markedly to the low spin side, causing a significant decrease of the magnetic moment and the average metal–ligand bond length. In FeP, which is normally pure high spin, the effect of included benzene is to induce a high spin ⇄ low spin equilibrium. The high spin form of FeP exhibits antiferromagnetic interactions which are shown to be diminished by increased separation of the complex molecules. This property of the $(t_2^3e^2)$ FeP is not shared to any significant extent by the isomorphous (t_2^3) CrP complex, and the e electrons therefore appear to be responsible for the bulk of the antiferromagnetic interactions.

ACKNOWLEDGMENT

Support received under NSF grants GP-16704 and GP-41679, and an instrumentation grant from Research Corporation, is gratefully acknowledged.

[1]A. H. White, R. Roper, E. Kokot, H. Waterman, and R. L. Martin, Aust. J. Chem. 17, 294 (1964), and references given therein.
[2]A. H. Ewald, R. L. Martin, E. Sinn, and A. H. White, Inorg. Chem. 8, 1837 (1969), and references cited therein.
[3]D. K. Straub and M. L. Epstein, Inorg. Chem. 8, 784 (1969).
[4]R. Rickards, C. E. Johnson, and H. A. O. Hill, J. Chem. Phys. 48, 5231 (1968); 51, 846 (1969).
[5]R. M. Golding, W. C. Tennant, J. P. M. Bailey, and A. Hudson, J. Chem. Phys. 48, 764 (1968).
[6]R. M. Golding, B. D. Lukeman, and E. Sinn, J. Chem. Phys. 56, 4147 (1972).
[7]L. G. Leipoldt and P. Coppens, Inorg. Chem. 17, 2269 (1973).
[8]P. C. Healy and E. Sinn, Inorg. Chem. 14, 109 (1975).
[9]R. J. Butcher and E. Sinn, J. Am. Chem. Soc. 98, 2440, 5159 (1976).
[10]G. R. Hall and D. N. Hendrickson, Inorg. Chem. 15, 607 (1976).
[11]R. J. Butcher, J. R. Ferraro, and E. Sinn, J. Chem. Soc. Chem. Commun. 1976, 910, Inorg. Chem. 15, 2077 (1976).
[12]S. Mitra, A. H. White, and C. L. Raston, Aust. J. Chem. 29, 1899 (1976).
[13]E. J. Cukauskas, B. S. Deaver, Jr., and E. Sinn, Bull. Am. Phys. Soc. 19, 229, 1120 (1974); J. Chem. Soc. Chem. Commun. 1974, 698; Inorg. Nucl. Chem. Lett. 13, 309 (1977).
[14]E. Sinn, Inorg. Chem. 15, 369 (1976).
[15]E. J. Cukauskas, D. A. Vincent, and B. S. Deaver, Jr., Rev. Sci. Instrum. 45, 83 (1974).
[16]A. H. Silver and J. E. Zimmerman, Phys. Rev. 157, 317 (1967).
[17]S. Foner, Rev. Sci. Instrum. 30, 548 (1959).
[18]R. M. Golding, P. C. Healy, P. W. G. Newman, E. Sinn, W. C. Tennant, and A. H. White, J. Chem. Phys. 52, 3105 (1970).
[19]M. Delepine, Bull. Soc. Chim. Fr. 3, 643 (1908).
[20]R. J. Butcher and E. Sinn, J. Chem. Soc. Dalton Trans. 1975, 2517.
[21]R. J. Butcher and E. Sinn (unpublished work).
[22]D. P. Freyberg, G. M. Mockler, and E. Sinn, J. Chem. Soc. Dalton Trans. 1976, 447.
[23]P. W. R. Corfield, R. J. Doedens, and J. A. Ibers, Inorg. Chem. 6, 197 (1967).
[24]D. T. Cromer and J. T. Waber, *International Tables for X-ray Crystallography* (Kynoch, Birmingham, 1974), Vol. IV.
[25]R. F. Stewart, E. R. Davidson, and W. T. Simpson, J. Chem. Phys. 42, 3175 (1965).
[26]D. T. Cromer and J. A. Ibers, Ref. 24.
[27]A table of structure factors for FeM·NBz has been deposited with AIP's Physics Auxiliary Publication Service (PAPS).
[28]R. M. Golding and H. J. Whitfield, Trans. Faraday Soc. 62, 1713 (1966).
[29]B. F. Hoskins and B. P. Kelley, Chem. Commun. 1517 (1968).
[30]G. C. Brackett, P. L. Richards, and W. S. Caughey, J. Chem. Phys. 54, 4383 (1971).
[31]P. C. Healy and A. H. White, J. Chem. Soc. Dalton Trans. 1972, 1163.
[32]R. M. Golding, C. R. Kanekar, R. L. Martin, and A. H. White, J. Chem. Phys. 45, 2688 (1966).
[33]R. M. Golding, P. C. Healy, P. Colombere, and A. H. White, Aust. J. Chem. 27, 2089 (1974).
[34]S. F. Krzeminski and D. K. Straub, J. Chem. Phys. 58, 1086 (1973).
[35]H. H. Wickman and C. F. Wagner, J. Chem. Phys. 51, 846 (1969).
[36]E. Sinn, Inorg. Chim. Acta 3, 11 (1969).
[37]G. P. Betteridge and R. M. Golding, J. Chem. Phys. 51, 2497 (1969).
[38]C. R. Kanekar, M. M. Dhingra, V. R. Marathe, and R. Nagarajan, J. Chem. Phys. 46, 2009 (1967).
[39]A. H. Ewald and E. Sinn, Aust. J. Chem. 21, 927 (1968).
[40]D. F. Lewis, S. J. Lippard, and J. A. Zubieta, Inorg. Chem. 11, 823 (1972).
[41]B. F. Hoskins and B. P. Kelley, Chem. Commun. 45, (1970).